Supporting Information for

Photoelectron-Photofragment Coincidence Studies of the Dissociation Dynamics of the OH-CH₄ Complex

Yanice Benitez,[1] Dandan Lu,[2] Katharine G. Lunny,[1] Jun Li,[2,3,*] Hua Guo,[4] and Robert E. Continetti[1,*]

[1]Department of Chemistry and Biochemistry, University of California, San Diego, 9500 Gilman Drive, La Jolla, CA 92093, USA

[2]School of Chemistry and Chemical Engineering, Chongqing University, Chongqing 401331, China

[3]Institut für Physikalische Chemie, Georg-August-Universität Göttingen, Göttingen 37077, Germany

[4]Department of Chemistry and Chemical Biology, University of New Mexico, Albuquerque, NM 87131, USA

*: corresponding authors, emails: jli15@cqu.edu.cn, rcontinetti@ucsd.edu

Contents

Figure S1. Schematic of source section comprising of the dual pulsed valve entrainment source, Wiley extraction plates, ion optics, COAT, and acceleration stack.

Figure S2. The geometries (distances in angstrom and angle in degree) and harmonic frequencies (cm^{-1}) of the optimized $OH^-(CH_4)$ anion. The first entry is obtained on the PIP-NN anion PES, and the second is determined at the level of CCSD(T)-F12a/AVTZ.

Figure S3. The fitting errors as a function of the ab initio energy (eV) for the anion PES with zero at the anion equilibrium.

Figure S4. The vibrational and rotational energy populations of the OH and CH_4

species.

Figure S5. Photoelectron-photofragment coincidence plot for $OH^-(CD_4)$. The KE_{max} for $OH + CD_4$ channel is labeled with a theoretical isotope shift of -0.0055 eV relative to the $OH^-(CH_4)$ KE_{max} for $OH + CH_4$.

Figure S6. Photoelectron-photofragment coincidence plot for $OD^-(CD_4)$. The KE_{max} for $OD + CD_4$ channel is labeled with a theoretical isotope shift of -0.0080 eV relative to the $OH^-(CH_4)$ KE_{max} for $OH + CH_4$.

Table S1. Dominant peak centers and their respective FWHMs for stable, dissociative, and total (stable + dissociative) photoelectrons.

Figure S1. Schematic of the source section comprising of the dual pulsed valve entrainment source, Wiley extraction plates, ion optics, COAT, and acceleration stack.
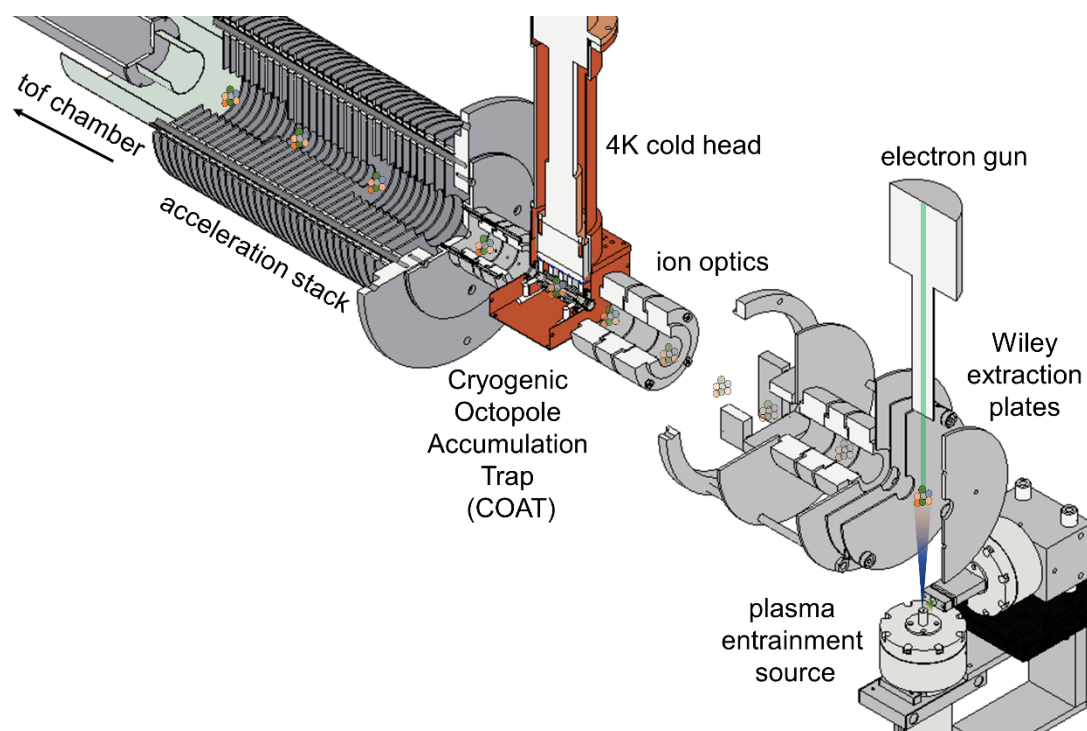
Figure S2. The geometries (distances in angstroms and angles in degrees) and harmonic frequencies (cm^{-1}) of the optimized OH$^-$(CH$_4$) anion. The first entry is obtained on the PIP-NN anion PES, and the second is determined at the level of CCSD(T)-F12a/AVTZ.

3775, 3093, 3089, 3056, 2897, 1575, 1573, 1374, 1374, 1291, 224, 218, 189, 101, 55
3772, 3099, 3095, 3057, 2902, 1574, 1572, 1378, 1376, 1283, 235, 233, 188, 123, 64
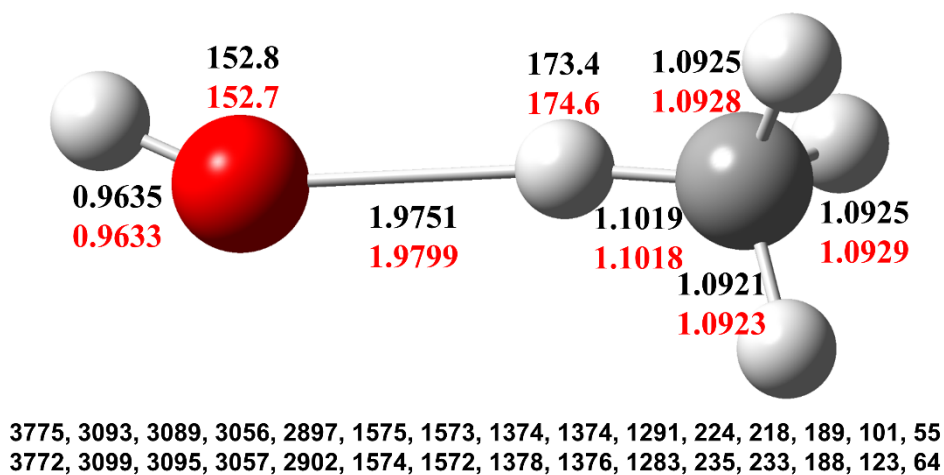
Figure S3. The fitting errors as a function of the ab initio energy (eV) for the anion
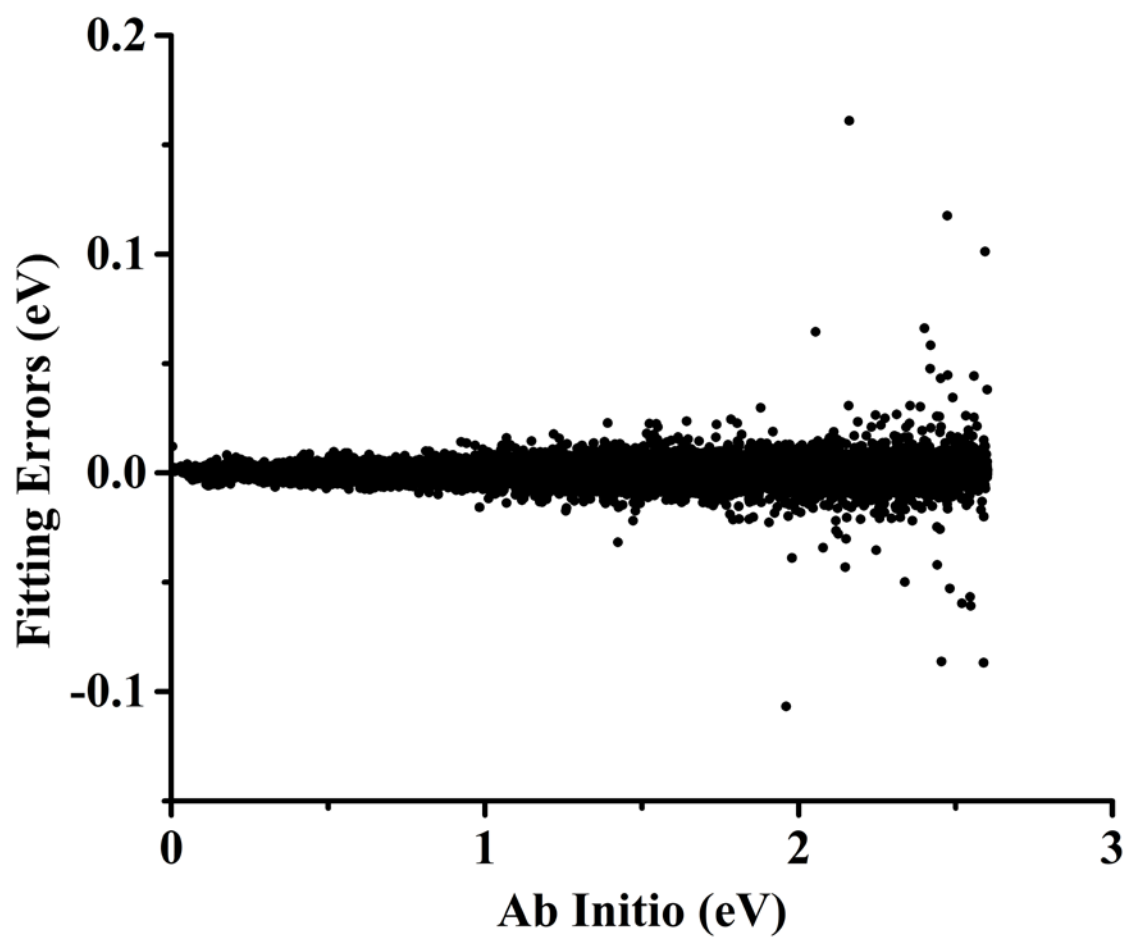
PES with zero at the anion equilibrium.

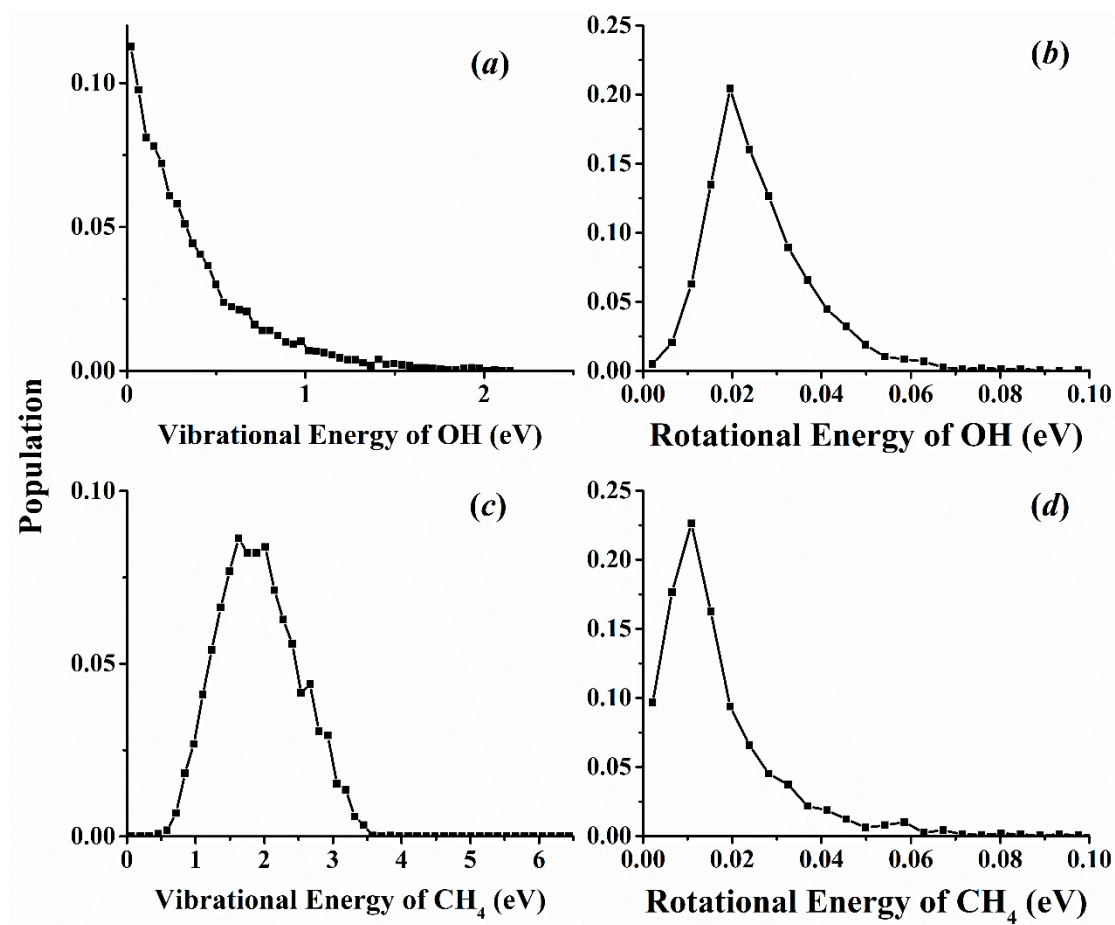**Figure S4**. The vibrational and rotational energy populations of the OH and CH4 species.

Figure S5. Photoelectron-photofragment coincidence plot for $OH^-(CD_4)$. The KE_{max} for $OH + CD_4$ channel is labeled with a theoretical isotope shift of -0.0055 eV relative to the $OH^-(CH_4)$ KE_{max} for $OH + CH_4$.

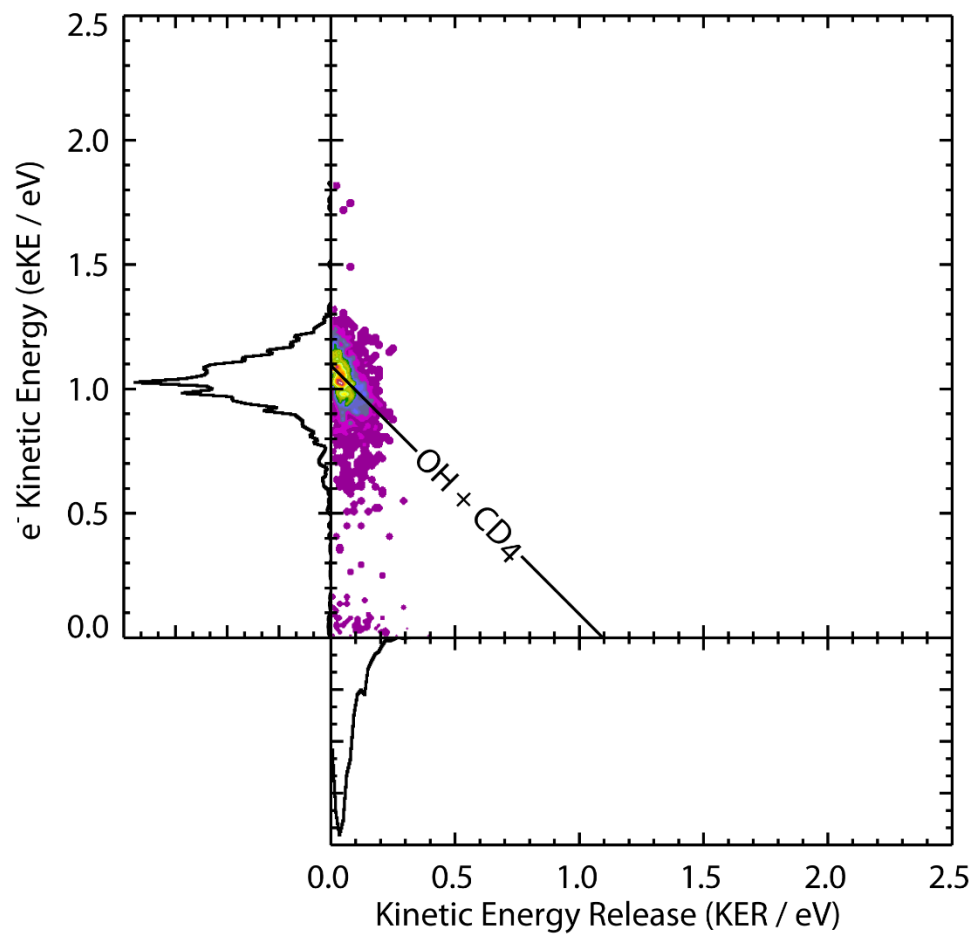**Figure S6**. Photoelectron-photofragment coincidence plot for $OD^-(CD_4)$. The KE_{max} for $OD + CD_4$ channel is labeled with a theoretical isotope shift of -0.0080 eV relative to the $OH^-(CH_4)$ KE_{max} for $OH + CH_4$.
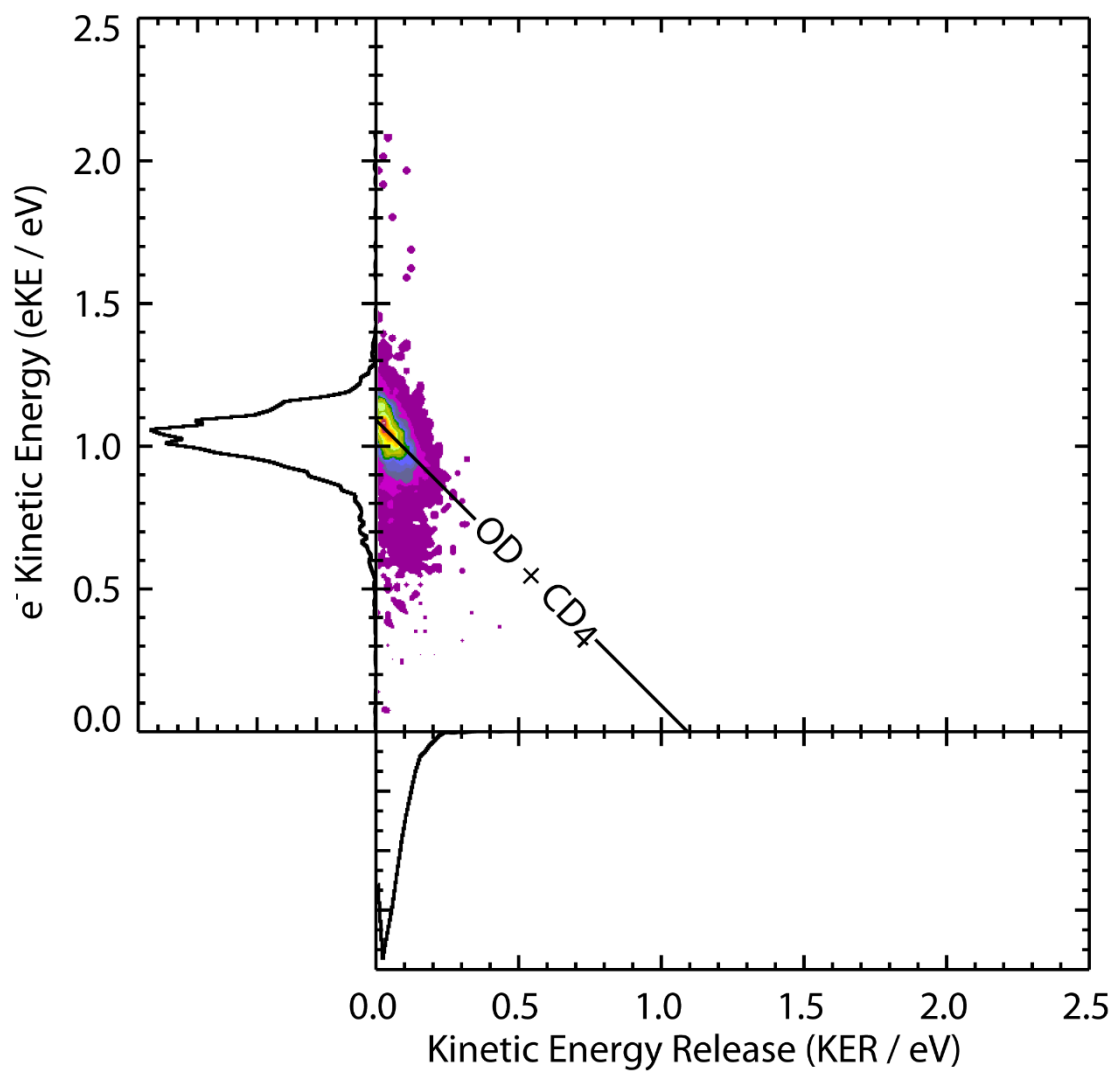
Table S1. Dominant peak centers and their respective FWHMs for stable, dissociative, and total (stable + dissociative) photoelectrons.

Species	eKE centers (eV)	FWHM (eV)
OH(CH$_4$)	1.09[a]	0.16
	1.03[b]	0.21
	1.06[c]	-
OH(CD$_4$)	1.10[a]	0.19
	1.03[b]	0.21
	1.06[c]	-
OD(CD$_4$)	1.10[a]	0.20
	1.04[b]	0.20
	1.05[c]	-

[a]Value for stable photoelectrons

[b]Value for dissociative photoelectrons

[c]Value for total (stable + dissociative) photoelectrons